

# MULTITUNABLE MICROWAVE SYSTEM FOR TOUCHLESS HEARTBEAT DETECTION AND HEART RATE VARIABILITY EXTRACTION

Dany Obeid,<sup>1</sup> Sawsan Sadek,<sup>2</sup> Gheorghe Zaharia,<sup>1</sup> and Ghaïs El Zein<sup>1</sup>

<sup>1</sup>IETR UMR CNRS 6164 – INSA, 20 Ave. des Buttes de Coësmes, CS 14315, 35043 Rennes, France; Corresponding author: dany.obeid@insa-rennes.fr

<sup>2</sup>Institut Universitaire de Technologie, Lebanese University, B.P. 813, Saida, Lebanon

Received 22 April 2009

**ABSTRACT:** This work proposes a contactless multitunable microwave measurement scheme for heartbeat detection. Our system is based on simplicity and the ability of tuning two parameters: frequency and power. Measurements are performed at 2.4, 5.8, 10, 16, and 60 GHz. Operating at 2.4 GHz, the heartbeat signal is detected at different output power levels (from  $-2$  down to  $-27$  dBm). The heart rate variability is extracted for all the measurements. © 2009 Wiley Periodicals, Inc. *Microwave Opt Technol Lett* 52: 192–198, 2010; Published online in Wiley InterScience (www.interscience.wiley.com). DOI 10.1002/mop.24877

**Key words:** microwave systems; doppler radar; heartbeat rate; heart rate variability; noncontact detection

## 1. INTRODUCTION

The demand for contactless heart monitoring has increased lately, especially for long duration monitoring and for patients with particular conditions, such as burn victims, or infants at risk of sudden infant syndrome. Based on the Doppler theory, a target with a periodic movement reflects the signal with its phase modulated by the time-varying position of the target [1]. Hence, the reflected signal of the person's chest contains information about the chest displacement, due to heartbeat and respiration. On the other hand, while holding breath, the reflected signal depends only on the chest displacement due to heartbeat. The chest displacement variation caused by respiration is between 4 mm and 12 mm [2]. However, the chest displacement due to heartbeat alone ranges between 0.2 mm and 0.5 mm [3]. This displacement is the concern of this work. Moreover, at rest, the frequency that corresponds to the respiration rate varies between 0.1 Hz and 0.3 Hz, whereas the frequency that corresponds to the heartbeat rate changes between 1 Hz and 3 Hz.

Previous work tended to detect life signs, respiration rates, and heartbeat rates, using a transmitted signal with fixed values of its frequency and power [4, 5]. Operating at 1.6 GHz and 2.4 GHz, direct-conversion Doppler radars have been integrated in 0.25  $\mu\text{m}$  CMOS and BiCMOS technologies [6]. Heart and respiration activities were detected using a modified Wireless Local Area Network PCMCIA card and a module combining the transmitted and reflected signals [7]. Other systems operating in the Ka-Band were described in [8, 9] using a low-power double-sideband transmission signal.

In this work, a new system for heartbeat detection is proposed with the ability of tuning both frequency and power. This feature is useful in determining the optimal frequency with the minimum transmitted power before the implementation process. This would be safer for both patients and medical staff. Experiments were performed at 2.4 GHz, 5.8 GHz, 10 GHz, 16 GHz, and 60 GHz. Also for a fixed frequency (2.4 GHz), measurements were performed at different power levels:  $-2$  dBm,

$-7$  dBm,  $-12$  dBm,  $-17$  dBm,  $-22$  dBm, and  $-27$  dBm. For all these experiments, the heartbeat rate and the heart rate variability (HRV) were extracted from the time domain variation of the phase of  $S_{21}$ , the forward complex transmission coefficient. The processing method for HRV extraction is applied to the original signal and the smoothed signal. The smoothing algorithm is based on the Newton's binomial. The rest of the article is organized as follows: Section 2 presents some background information. Section 3 describes briefly the main features of the proposed system. Sections 4 and 5 present the results for different frequency bands and power levels, respectively. Section 6 concludes the work.

## 2. BACKGROUND INFORMATION

In normal cases, the respiration rate varies between 10 and 18 breaths per minute, which corresponds to a frequency between 0.1 Hz and 0.3 Hz. At rest, adults' heartbeats rate ranges from 60 to 120 beats per minute; this corresponds to a frequency between 1 Hz and 2 Hz. The average chest displacement, caused by a heartbeat, ranges between 0.2 mm to 0.5 mm. The peak-to-peak chest motion, caused by respiration, varies from 4 mm to 12 mm. The phase of the reflected signal off the person's chest is directly proportional to the chest motion and is scaled by the wavelength of the signal. The relation between the chest displacement and the phase variation is:

$$\Delta\theta(t) = \frac{4\pi\Delta x(t)}{\lambda}, \quad (1)$$

where  $\Delta x(t)$  is the chest displacement and  $\lambda$  is the wavelength of the transmitted signal.

Normally, an electrocardiogram (ECG), obtained with fixed electrodes on the chest and limbs, measures the electrical current generated in the extracellular fluid, due to changes in the membrane potential across many cells in the heart; thus giving information about the heart activity. An exemplary output is shown in Figure 1. The *P* wave shows the current flow during atria depolarization, which triggers the atria to contract. The ventricular depolarization, which triggers the ventricles to contract, is represented as the QRS complex. The *T* wave shows ventricular repolarization. The R–R interval is the duration of the ventricular cardiac cycle; in other words, each R-peak corresponds to a single heartbeat. The HRV is a measure of the beat-to-beat variations (R–R interval). HRV is regarded as an activity indicator of autonomic regulation of circulatory function; notice that controversy exists over whether this is an accurate metric for analyzing cardiovascular autonomic control [10, 11]. A simple example of information extraction in time domain is the calculation of the standard deviation (STD) of beat-to-beat intervals [12]. The intervals between heart beats can be statistically analyzed to obtain information about the autonomic nervous system [13].

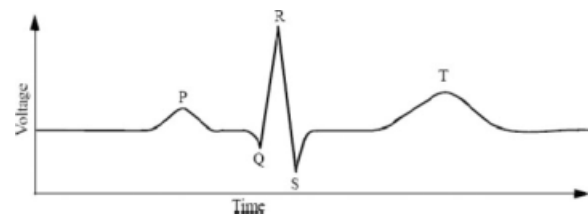


Figure 1 Electrocardiogram exemplary output

In this work, the HRV is extracted in the time domain and the STD is calculated.

### 3. SYSTEM DESCRIPTION

The proposed system is based on using a Vector Network Analyzer (VNA) (Agilent N5230A 4-Port) operating up to 20 GHz and two horn antennas. It is worth mentioning that many features are accessible by using a VNA, such as choosing the sweep time and the number of measurement points; therefore, the sampling rate. Here, the frequency and the transmitted power can be set and modified manually, and the time variation of the phase of the transmission coefficient  $S_{21}$ , can be measured. Measurements are taken at several frequencies: 2.4 GHz, 5.8 GHz, 10 GHz, and 16 GHz. Both horn antennas have the following characteristics:

- Frequency: 2–18 GHz
- Nominal gain: from 10 to 22 dBi
- Half power beamwidth: from  $60^\circ$  to  $11^\circ$
- VSWR < 2.5:1
- Dimensions:  $622 \times 165 \times 165 \text{ mm}^3$

Because of the limited frequency (20 GHz) of the VNA, an up-conversion method is used to achieve 60 GHz frequency.

The measurement setup has the following characteristics:

- Sweep time: 10 s
- Measurement points: 20,000

- Sampling frequency: 1000 Hz
- Total output power (output power of the VNA + antenna gain): from  $-2 \text{ dBm}$  down to  $-27 \text{ dBm}$

The VNA generates a continuous wave (CW) signal at the desired frequency. The reflected signal of the person's chest is received by the antenna and fed back into the VNA, where the phase of  $S_{21}$  is computed. This phase corresponds to the difference between the phase of the received and the transmitted signal. The proposed system is described in details in [14].

### 4. HEARTBEAT DETECTED AT DIFFERENT FREQUENCIES

At a distance of 1 m from a 27-years-old person, and at  $-10 \text{ dBm}$  total output power, our system was used at different frequencies: 2.4 GHz, 5.8 GHz, 10 GHz, 16 GHz, and 60 GHz. The heartbeat signal detected at 2.4 GHz is shown in Figure 2(a), in which a phase variation of  $1.57^\circ$  is observed. The heartbeat signal detected at 5.8 GHz is shown in Figure 2(b), in which a phase variation of  $3.66^\circ$  is observed. Operating at 10 GHz, our proposed system indicates a phase variation of  $5.27^\circ$  as shown in Figure 2(c). Operating at 16 GHz, our proposed system indicates a phase variation of  $10.46^\circ$  as shown in Figure 2(d). The heartbeat signal detected using 60 GHz signal is presented in Figure 2(e), in which a phase variation of  $43.85^\circ$  is observed. Higher sensitivity to small displacements is obtained at higher frequencies. In addition, the difference in the phase variation due to heartbeat, detected at different frequencies, is shown in Figure 2(f), in which the heartbeat signals for different

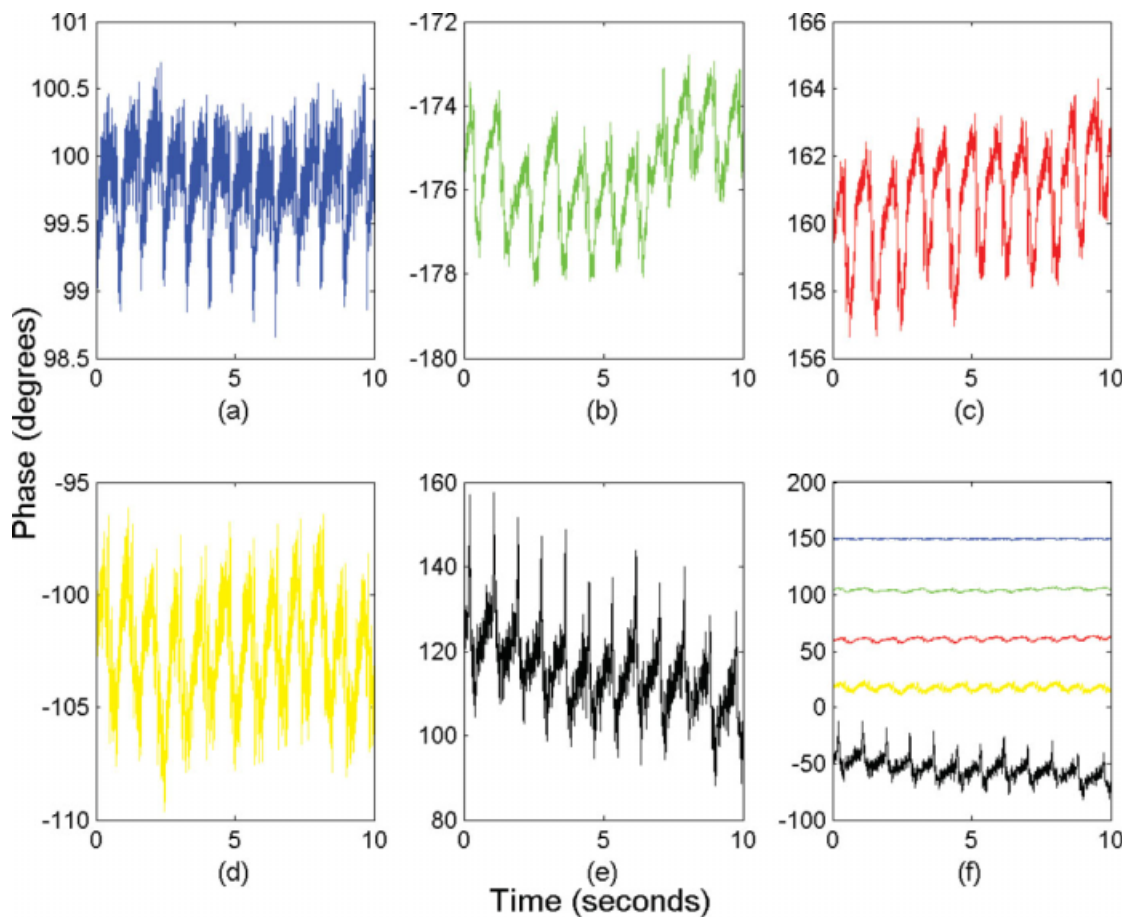


**Figure 2** Heartbeat signal detected at 2.4 GHz (a), 5.8 GHz (b), 10 GHz (c), 16 GHz (d), and 60 GHz (e). [Color figure can be viewed in the online issue, which is available at [www.interscience.wiley.com](http://www.interscience.wiley.com)]

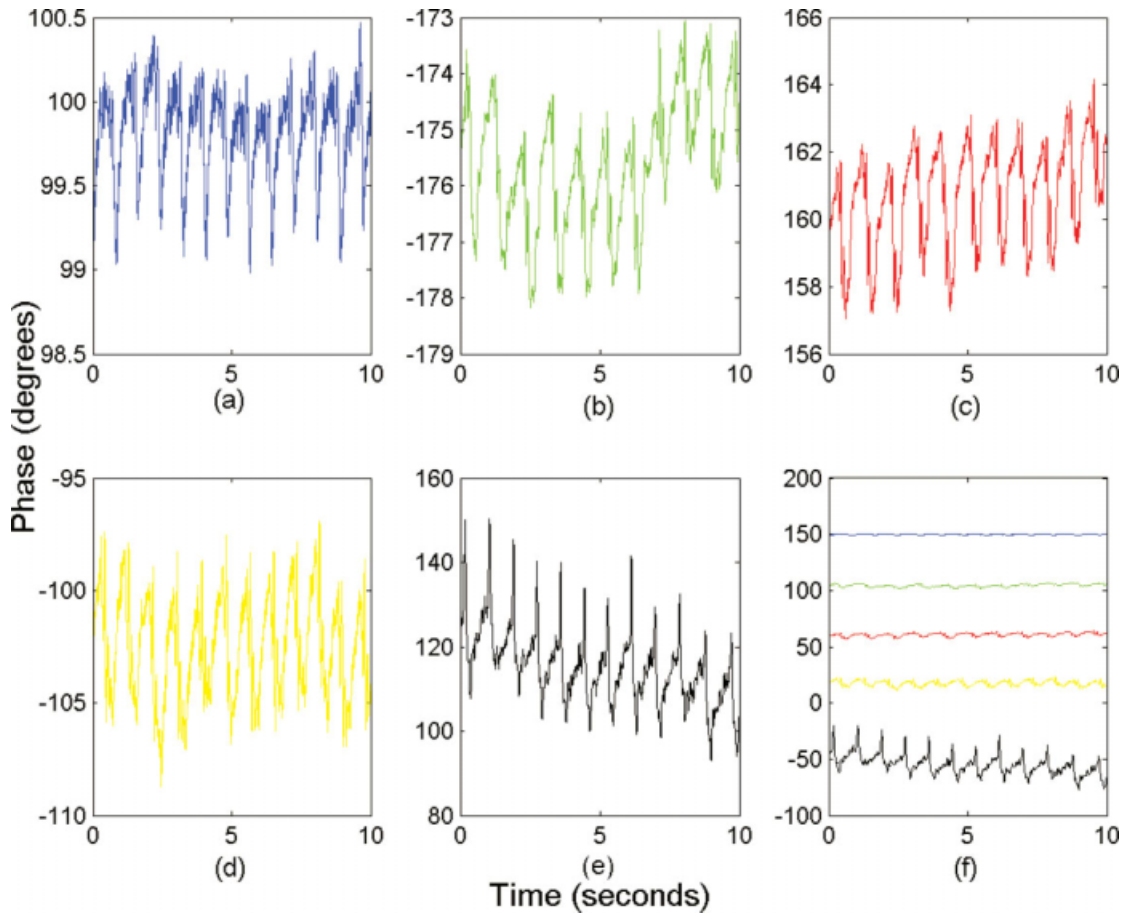


**Figure 3** Smoothed heartbeat signal detected at 2.4 GHz (a), 5.8 GHz (b), 10 GHz (c), 16 GHz (d), and 60 GHz (e). [Color figure can be viewed in the online issue, which is available at [www.interscience.wiley.com](http://www.interscience.wiley.com)]

frequencies are plotted within the same scale. From top to bottom, Figure 2(f) shows the heartbeat signal detected from 2.4 GHz and up to 60 GHz.

As the heartbeat rate is based on the detection of the signal peaks, a smoothing method is applied to reduce the number of surrounding peaks. The smoothing method is based on the Newton relation:

$$(a + b)^n = \sum_{k=0}^n C_n^k a^{n-k} b^k, \quad (2)$$

where  $n + 1$  ( $n = 2m$ , where  $m$  is an integer number) is the length of the smoothing window. In this case, the phase  $p(i)$  is replaced by the weighted mean of the values:  $p(i - m) \dots p(i + m)$ . The weighting coefficients are given by the Newton binomial [2]. In this work,  $n$  is chosen to be 10.

The effect of smoothing the signal is shown in Figure 3. Figures 3(a)–3(e) show, respectively, the smoothed heartbeat signal

detected at 2.4 GHz, 5.8 GHz, 10 GHz, 16 GHz, and 60 GHz. Because of the smoothing method, the phase variations of the heartbeat signal detected at the experimented frequencies are decreased by about 20%. Table 1 shows the theoretical and the experimental results for the chest-wall displacement: based on Eq. (1), the phase variations due to the limits of the chest displacement (0.2 mm to 0.5 mm), caused by heart-beatings, are presented for all the utilized frequencies. Experimental phase variations for both, the original signal and the smoothed signal are also presented for all the frequencies.

For the 10-s duration of each experiment, the heartbeat rate is calculated for both the original signal and the smoothed signal, as shown in Table 2. As the phase variation is smaller at lower frequencies than at higher frequencies, it is more effective to smooth the signal at the former. However, the difference in the heartbeat rate between the original and the smoothed signal is considerably small. As presented in Table 2, the heartbeat rate computed from the signal detected at 2.4 GHz varies after

**TABLE 1** Phase Variation of the Chest Displacement due to Heart-Beating: Theoretical and Experimental Values

Frequency (GHz)	$\lambda$ (mm)	$\Delta\theta$ for $\Delta x = 0.2$ mm	$\Delta\theta$ for $\Delta x = 0.5$ mm	Experimental Phase Variation of the Original Signal	Experimental Phase Variation of the Smoothed Signal
2.4	125	1.15°	2.88°	1.57°	1.11°
5.8	51.72	2.78°	6.96°	3.66°	3.28°
10	30	4.8°	12°	5.27°	4.72°
16	18.75	7.68°	19.2°	10.46°	8.28°
60	5	28.8°	72°	43.85°	32.85°

**TABLE 2 Heartbeat Rate and the Standard Deviation of the HRV for Both the Original and the Smoothed Signals for Different Frequencies**

Frequency (GHz)	Heartbeat Rate (beats/min)			STD of the HRV		
	Original Signal	Smoothed Signal	Relative Error (%)	Original Signal	Smoothed Signal	Relative Error (%)
2.4	78.67	75.39	4.16	0.2210	0.1740	21.26
5.8	71.03	70.68	0.49	0.0696	0.0601	14.64
10	66.74	66.66	0.12	0.1102	0.1031	6.44
16	62.31	62.36	0.08	0.0536	0.0531	0.93
60	69.26	69.24	0.03	0.0364	0.0367	0.82

smoothing by 3 beats/min, corresponding to 4.16% relative error. The relative error is calculated with respect to the original signal. The heartbeat rate of the signal detected at 5.8 GHz varies after smoothing by 1 beat/min, corresponding to 0.49% relative error. On the other hand, the variation of the heartbeat rate between the original signal and the smoothed signal is less than 1 beat/min, when operating at 10 GHz, 16 GHz, and 60 GHz with a relative error of 0.12%, 0.08%, and 0.03%, respectively.

Another important variable extracted in this work is the heart rate variability. The HRV analysis is based on the variations in the instantaneous heartbeat rate, using the beat-to-beat RR-intervals. Figures 4(a)–4(e) show, respectively, the HRV of the heartbeat signal detected at 2.4 GHz, 5.8 GHz, 10 GHz, 16 GHz, and 60 GHz, and for both the original signal and the smoothed signal. The STD for each HRV is calculated and shown in Table 2.

The difference in the STD of the HRV between the original and the smoothed signal is less at higher frequencies than at lower frequencies. As previously mentioned, smoothing the signal has more effects at signals detected at lower frequencies than at signals detected at higher frequencies; this is due to the phase variation that depends on the wavelength of the transmitted signal as shown by [1]. As the HRV extraction is based on the detection of the signal peaks (corresponding to R-peaks), the peak position may be changed after smoothing. Hence, the difference in the STD of the HRV between the original and the smoothed signal is less at higher frequencies. The relative error in the STD of the HRV, between the original signal and the smoothed signal, is 21.26% when operating at 2.4 GHz, 14.64% when operating at 5.8 GHz, 6.44% when operating at 10 GHz, 0.93% when operating at 16 GHz, and 0.82% when operating at 60 GHz.

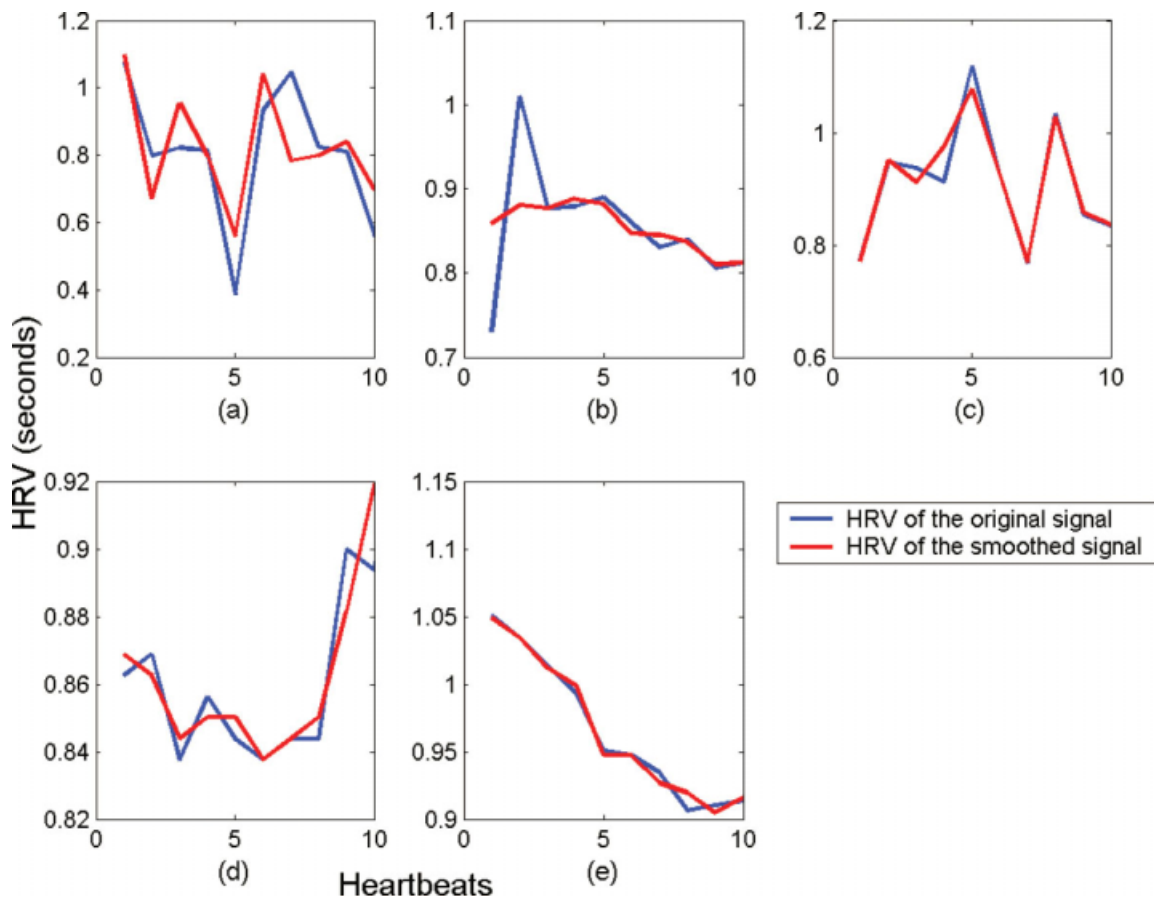


**Figure 4** HRV of both the original and the smoothed heartbeat signals detected at 2.4 GHz (a), 5.8 GHz (b), 10 GHz (c), 16 GHz (d), and 60 GHz (e). [Color figure can be viewed in the online issue, which is available at [www.interscience.wiley.com](http://www.interscience.wiley.com)]

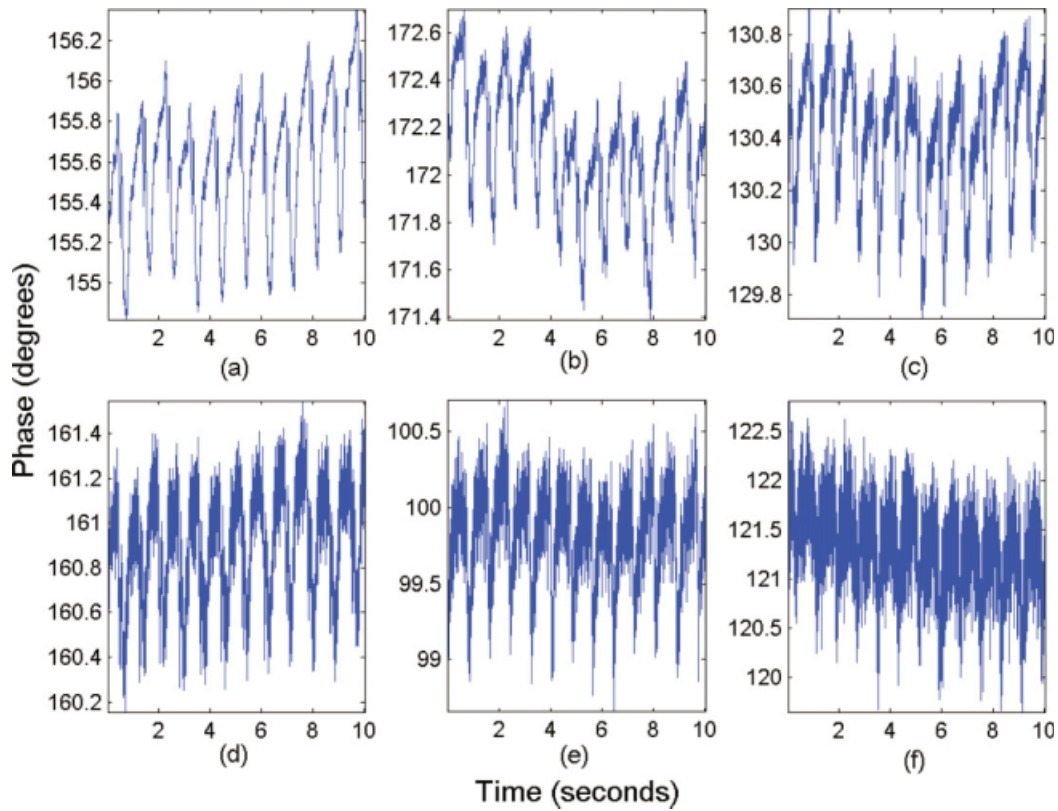


**Figure 5** Heartbeat signal detected at 2.4 GHz for different power levels:  $-2$  dBm (a),  $-7$  dBm (b),  $-12$  dBm (c),  $-17$  dBm (d),  $-22$  dBm (e), and  $-27$  dBm (f). [Color figure can be viewed in the online issue, which is available at [www.interscience.wiley.com](http://www.interscience.wiley.com)]

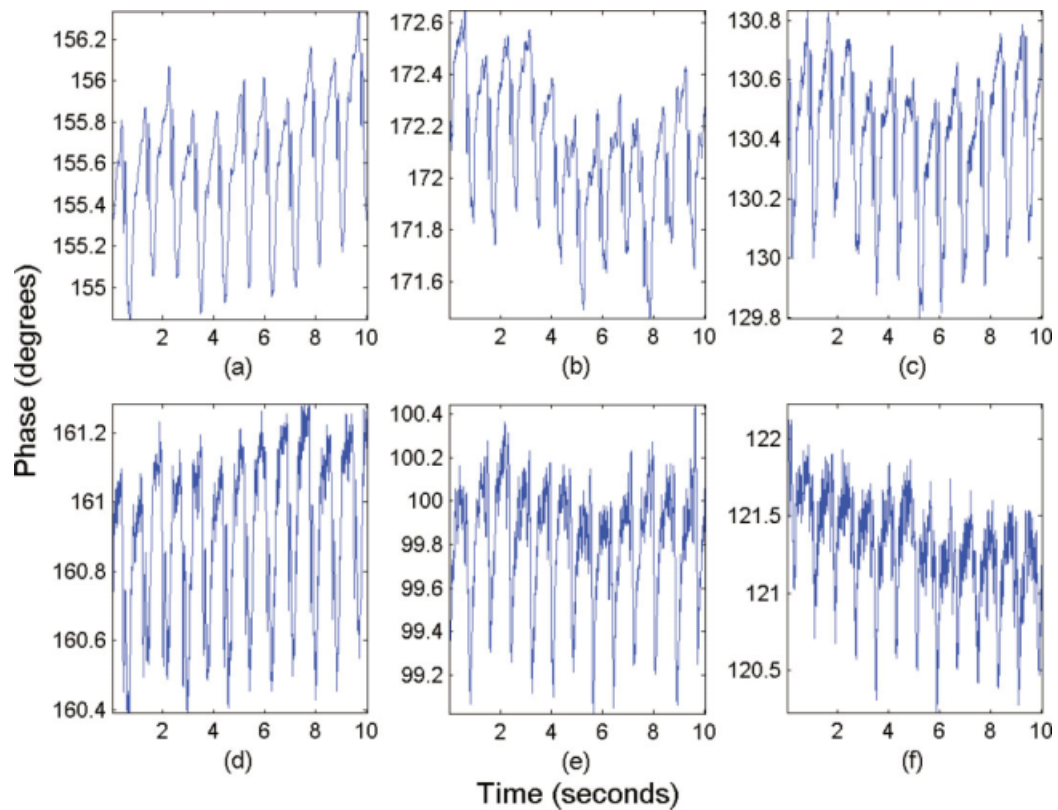


**Figure 6** Smoothed heartbeat signal detected at 2.4 GHz for different power levels:  $-2$  dBm (a),  $-7$  dBm (b),  $-12$  dBm (c),  $-17$  dBm (d),  $-22$  dBm (e), and  $-27$  dBm (f). [Color figure can be viewed in the online issue, which is available at [www.interscience.wiley.com](http://www.interscience.wiley.com)]

**TABLE 3 Heartbeat Rate and the Standard Deviation of the HRV for Both the Original and the Smoothed Signals, Detected at 2.4 GHz, for Different Power Levels**

Power (dBm)	Heartbeat Rate (beats/min)			STD of the HRV		
	Original Signal	Smoothed Signal	Relative Error (%)	Original Signal	Smoothed Signal	Relative Error (%)
-2	79.97	79.96	0.0125	0.0497	0.0493	0.65
-7	88.01	87.84	0.19	0.1699	0.1677	1.27
-12	64.57	64.90	0.51	0.0603	0.0700	16.15
-17	79.51	78.21	1.63	0.1617	0.1318	18.50
-22	78.57	74.29	5.44	0.2134	0.1700	20.33
-27	88.17	81.42	7.66	0.1953	0.1550	20.63

**5. HEARTBEAT DETECTED AT DIFFERENT POWER LEVELS**

Nowadays, one of the main contributions is decreasing the power of the transmitted signal. The less the power, the safer the system is for both patients and medical staff. Operating at 2.4 GHz, our system shows capability of detecting body motions due to heart-beating at total transmitted power as low as -27 dBm; this value corresponds to the generated power of the VNA (-40 dBm) added to the antenna gain (~13 dB). Starting at -2 dBm, and decreasing the power by 5 dB, down to -27 dBm, our system still detects the heart activity, as shown in Figure 5. Figures 5(a)–5(f) show, respectively, the heartbeat signal detected using 2.4 GHz at -2 dBm, -7 dBm, -12 dBm, -17 dBm, -22 dBm, and -27 dBm. The smoothed signals are shown in Figure 6. The heartbeat rate is calculated for each heartbeat signal (original and smoothed). At -2 dBm, -7 dBm,

and -12 dBm, the difference in the heartbeat rate between the original signal and the smoothed signal is less than 1 beat/min, which corresponds to a relative error less than 1%. However, at -17 dBm, the difference in the heartbeat rate, between the original signal and the smoothed signal, is less than 2 beats/min; and the relative error is 1.63%. At -22 dBm, the difference in the heartbeat rate, between the original signal and the smoothed signal, is less than 5 beats/min; the relative error being here 5.44%. On the other hand, the difference in the heartbeat rate, between the original signal and the smoothed signal, is less than 7 beats/min when operating at -27 dBm; with a relative error of 7.66%. The heartbeat rates of the signal detected at 2.4 GHz are shown in Table 3, for the original signal and the smoothed signal, at all the power levels. The HRV is extracted for both the original signal and the smoothed signal. Figures 7(a)–7(f)

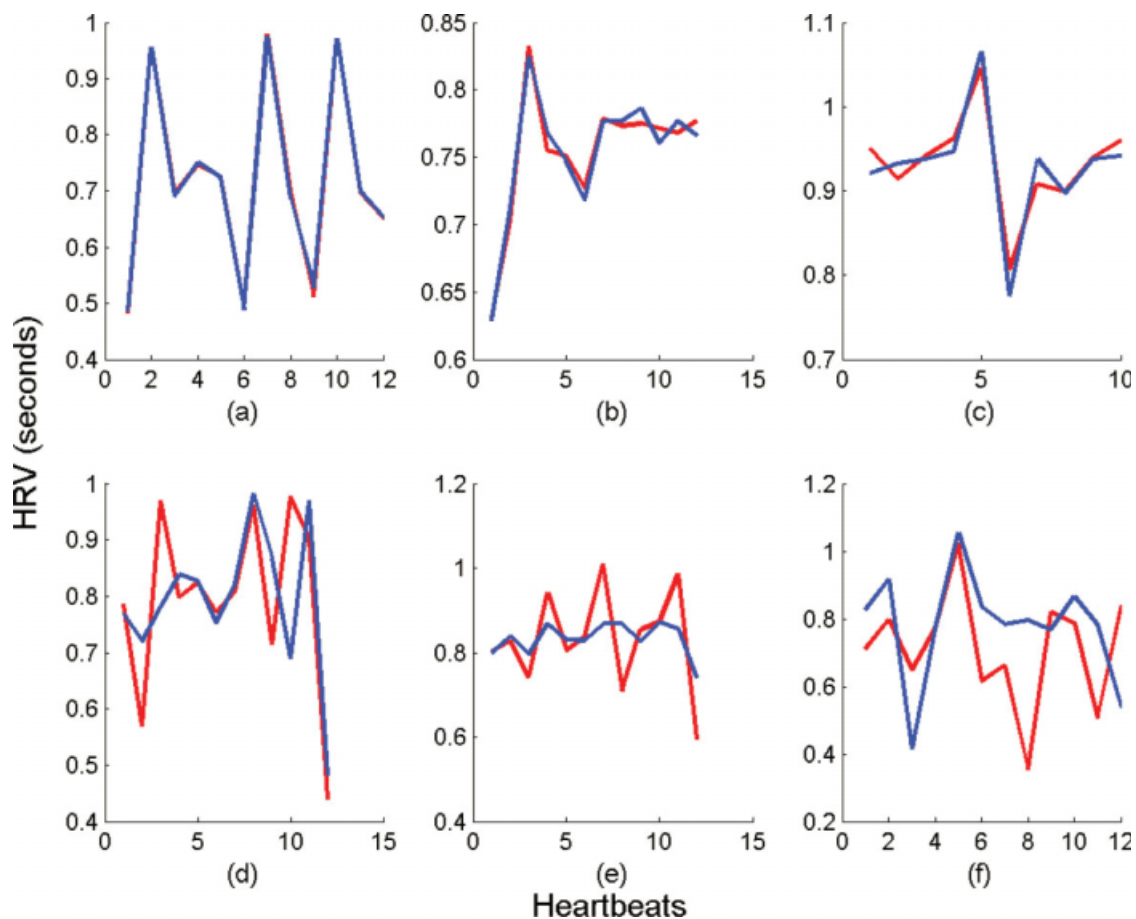


**Figure 7** HRV of both the original and the smoothed heartbeat signals detected at 2.4 GHz for different power levels: -2 dBm (a), -7 dBm (b), -12 dBm (c), -17 dBm (d), -22 dBm (e), and -27 dBm (f). [Color figure can be viewed in the online issue, which is available at [www.interscience.wiley.com](http://www.interscience.wiley.com)]

show, respectively, the HRV of signal detected at  $-2$  dBm,  $-7$  dBm,  $-12$  dBm,  $-17$  dBm,  $-22$  dBm, and  $-27$  dBm. The STD of each of these HRVs is calculated and stated in Table 3. The relative error in the STD of the HRV, between the original signals and the smoothed signals, is 0.65% when the total output power is  $-2$  dBm, 1.27% when the total output power is  $-7$  dBm, 16.15% when the total output power is  $-12$  dBm, 18.5% when the total output power is  $-17$  dBm, 20.33% when the total output power is  $-22$  dBm, and 20.63% when the total output power is  $-27$  dBm. This demonstrates the ability of the proposed system to detect the heartbeat rate and the HRV at power levels as low as  $-27$  dBm.

## 6. CONCLUSION

At a distance of 1 m from a 27-years-old person, our system was used with the variation of two parameters: frequency and power. At a total output power of  $-10$  dBm, the heartbeat signal was detected at several frequencies: 2.4 GHz, 5.8 GHz, 10 GHz, 16 GHz, and 60 GHz. As expected, higher sensitivity to small displacements is observed at higher frequencies. Operating at 2.4 GHz, the heartbeat signal was detected at  $-2$  dBm,  $-7$  dBm,  $-12$  dBm,  $-17$  dBm,  $-22$  dBm, and  $-27$  dBm. The ability to detect the heartbeat signal at a distance of 1 m with a total output power of  $-27$  dBm can put forth new safer techniques for both patients and medical staff. For all performed experiments, the heartbeat rate, the HRV, and the STD of the HRV were extracted. Our system shows simplicity in terms of installation and incorporates the ability of tuning both frequency and power.

Our future work will focus on determining the optimum frequency for the minimum possible transmitted power.

## ACKNOWLEDGMENTS

The authors acknowledge CEDRE for partially funding this work (project reference number: 08Sci F6/L4).

## REFERENCES

- J.C. Lin, Microwave sensing of physiological movement and volume change: A review, *Bioelectromagnetics* 13 (1992), 557–565.
- A. DeGroote, M. Wantier, G. Cheron, M. Estennes, and M. Pavia, Chest wall motion during tidal breathing, *J Appl Physiol* 83 (1997), 1531–1537.
- G. Ramachandran and M. Singh, Three-dimensional reconstruction of cardiac displacement patterns on the chest wall during the P, QRS, and T-segments of the ECG by laser speckle interferometry, *Med Biol Eng Comput* 27 (1989), 525–530.
- K.M. Chen, Y. Huang, J. Zhang, and A. Norman, Microwave life-detection systems for searching human subjects under earthquake rubble and behind barrier, *IEEE Trans Biomed Eng* 47 (2000), 105–114.
- A.D. Droitcour, V.M. Lubecke, J. Lin, and O. Boric-Lubecke, A microwave radio for Doppler radar sensing of vital signs, *IEEE MTT-S Int Microw Symp Dig*, Phoenix, AZ (2001), 175–178.
- A.D. Droitcour, O. Boric-Lubecke, V.M. Lubecke, and J. Lin, 0.25 mm CMOS and BiCMOS single chip direct conversion Doppler radars for remote sensing of vital signs, *IEEE International Solid-State Circuits Conference Technology Digest*, San Francisco, CA, Feb. 2002, pp. 348–349.
- O. Boric-Lubecke, G. Awater, and V.M. Lubecke, Wireless LAN PC card sensing of vital signs, *IEEE Top Conf Wireless Commun Technol* (2003), 206–207.
- Y. Xiao, J. Lin, O. Boric-Lubecke, and V.M. Lubecke, A Ka-band low power Doppler radar system for remote detection of cardiopulmonary motion, Presented at the 27th IEEE Annual Engineering Medical and Biological Society Conference, Sep. 1–4, 2005.
- Y. Xiao, J. Lin, Boric-Lubecke, and V.M. Lubecke, Frequency tuning technique for remote detection of heartbeat and respiration using low-power double-sideband transmission in Ka-band, *IEEE Trans Microw Theory Tech* 54 (2006), 2023–2032.
- P. Joseph, U.R. Acharya, C.K. Poo, J. Chee, L.C. Min, S.S. Iyengar, and H. Wei, Effect of reflexological stimulation on heart rate variability, *ITBM-RBM* 25 (2004), 40–45.
- D.C. Lin and R.L. Hughson, Modeling heart rate variability in healthy humans: A turbulence analogy, *Phys Rev Lett* 86 (2001), 1650–1653.
- A. Al-Hazimi, N. Al-Ama, A. Syiamic, R. Qosti, and K. Abdel-Galil, Time domain analysis of heart rate variability in diabetic patients with and without autonomic neuropathy, *Ann Saudi Med*, 22 (2002), 400–403.
- E. Gil, M.O. Mendez, O. Villantieri, J. Mateo, J.M. Vergara A. M. Bianchi, and P. Laguna, Heart rate variability during pulse photoplethysmography decreased amplitude fluctuations and its correlation with apneic episodes, *Comput Cardiol* 33 (2006), 165–168.
- D. Obeid, S. Sadek, G. Zaharia, and G. El-Zein, Non-contact heartbeat detection at 2.4, 5.8 and 60 GHz: A comparative study, *Micro-wave Opt Technol Lett* 51 (2009), 666–669.

© 2009 Wiley Periodicals, Inc.

## A COMPACT MODIFIED MONOPOLE TYPE INTERNAL ANTENNA FOR WIRELESS USB DONGLE APPLICATION

Yeonsik Yu and Jaehoon Choi

Department of Electrical and Computer Engineering, Hanyang University, 17 Haengdang-Dong, Seongdong-Gu, Seoul 133-791, Korea; Corresponding author: choihj@hanyang.ac.kr

Received 22 April 2009

**ABSTRACT:** Proposed within this document is a compact internal antenna intended for multiband operation. The antenna consists of two-pronged elements with two stubs and has a comparatively small volume of  $16 \text{ mm} \times 5 \text{ mm} \times 1 \text{ mm}$ . The measured return loss of the designed antennas was  $>10$  dB for wireless broadband (WiBro), wireless local area network (WLAN), world interoperability for microwave access (WiMAX), and satellite digital multimedia broadcast (S-DMB) frequency bands. A high-quality radiation pattern and a reasonable antenna efficiency were obtained within the desired frequency band. © 2009 Wiley Periodicals, Inc. *Microwave Opt Technol Lett* 52: 198–201, 2010; Published online in Wiley InterScience (www.interscience.wiley.com). DOI 10.1002/mop.24878

**Key words:** modified monopole; internal antenna; USB dongle application

## 1. INTRODUCTION

Many portable device users want efficient and uncomplicated access to their favorite services at any time or place. However, it is currently impossible to provide all of the recently emerging services, such as, high-quality multimedia broadcasting and wireless internet, with a single-digital device. The conventional universal serial bus (USB) is used for information exchange within most digital devices, including mobile phones, portable multimedia players (PMP), personal digital assistants (PDA), and laptops, because it provides high-quality connectivity through a simple “plug and play” function [1]. A USB dongle is very adaptable because it can be integrated not only with an antenna, in order to achieve various wireless communications, but also with an existing device, which decreases the necessity for purchasing a new digital device. Reports have been